EUROFUSION WPMAG-CP(16) 15415

A. Brighenti et al.

Analysis of partial blockage of the coolant in a TF coil of the EU DEMO

Preprint of Paper to be submitted for publication in Proceedings of 29th Symposium on Fusion Technology (SOFT 2016)

This work has been carried out within the framework of the EUROfusion Consortium and has received funding from the Euratom research and training programme 2014-2018 under grant agreement No 633053. The views and opinions expressed herein do not necessarily reflect those of the European Commission.

Performance analysis of a graded winding pack design for the EU DEMO TF coil in normal and off-normal conditions

Laura Savoldi[a] *, *Member, IEEE,* Alberto Brighenti[a], Roberto Bonifetto[a], Valentina Corato[b], Luigi Muzzi[b,c], *Senior Member, IEEE,* Simonetta Turtù[b,c], *Senior Member, IEEE*, Roberto Zanino[a], *Senior Member, IEEE*

[a] NEMO Group, Dipartimento Energia, Politecnico di Torino, Italy
[b] ENEA, Frascati, Italy
[c] ICAS, Frascati, Italy

Abstract

The superconducting magnet system plays an important role in the framework of the design of the EU DEMO tokamak. In recent years, ENEA developed a prototype of cable-in-conduit conductor (CICC) with two low-impedance central channels to be used in the DEMO Toroidal Field (TF) coils with a graded winding pack (WP). In this paper, a model of a TF coil based on the thermal-hydraulic code 4C has been developed, including the WP, the steel casing with dedicated cooling channels (CCCs) and the two independent cryogenic circuits cooling the WP and the casing, respectively. The first part of the work analyzes the performance of the WP during a series of standard plasma pulses in normal operating conditions. In the second part different off-normal operating conditions during the plasma pulses are studied, namely the collapse of one or both central channel(s) in the most critical CICCs and the plugging of some CCCs at the most critical locations in the magnet.

Keywords: nuclear fusion, EU DEMO, superconducting magnets, DC performance, thermal-hydraulic analysis

1. Introduction

In the frame of the EU DEMO design activities [1], a big effort is being devoted in the Work Package Magnets (WPMAG) to the preliminary design of the Toroidal Field (TF) coils, resulting in the proposal of three different conductors and corresponding winding packs (WPs) by different European institutions [2], [3]. These proposals are periodically updated and optimized taking into account the feedback from mechanical and thermal-hydraulic (TH) analyses, as well as, of course, the updates in the input form the EUROfusion Project Management Unit.

The TH code 4C [4] was already used to develop the first model of an entire EU DEMO TF coil, including structures and a simple cooling circuit, [5] and applied, with the addition of quench lines in the model, to the quench analysis of the magnet [6]. In this paper, the previous model is updated to the new WP and conductor designs proposed by ENEA after the 2015 DEMO design review that increased the number of TF coil from 16 to 18 [7]. The model is then used first to assess the coil DC performance, considering, as a major difference with past works analyzing steady state burns [5], [8], [9], the standard pulsed operation currently foreseen for DEMO: several cycles are simulated, up to a periodic behavior of the coil. The value (and location) of the minimum temperature margin (ΔT_{marg}^{min}) in the WP is computed and compared with the minimum acceptable value of 1.5 K [10]. The study is then repeated in off-normal conditions, i.e. considering the choking of the flow in the pressure relief channels of the most critical conductor or in some casing cooling channels (CCCs).

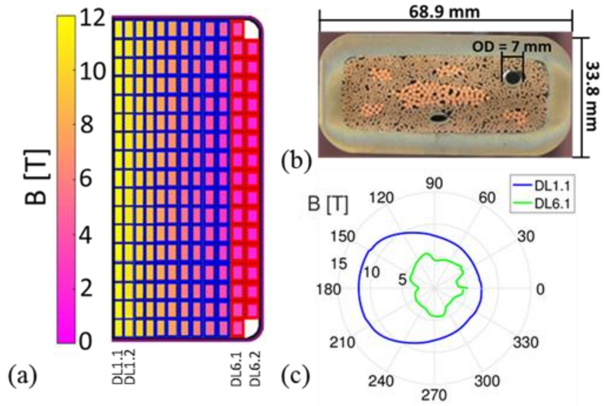

Fig. 1. (a) ENEA 2016 design of the TF WP with six DLs including Nb_3Sn (blue) and NbTi (red) conductors. The 2D magnetic field amplitude map on the inboard equatorial cross section is reported (the plasma is on the left). (b) Cross section of the ENEA conductor concept on which 2016 WP design is based. (c) Polar distribution of the magnetic field amplitude in the central turn of DL1.1 (blue) and in the last turn of DL6.1 (green), at nominal operating current; the inboard equatorial plane is at 180°.

2. Conductor and WP

The most recent WP proposal by ENEA (the so-called WP2016#2) is an upgrade of the 2015 design [11] and consists of a double-layer (DL) wound WP, see

Corresponding author: laura.savoldi@polito.it

Table 1. Main geometrical parameters EU DEMO TF WP2016 by ENEA. Where different, the values for the first and second layer of the same DL are separated by "/".

	Nb_3Sn					NbTi
	DL1	DL2	DL3	DL4	DL5	DL6
N. SC strands (D=1 mm)	720	360	270	180	120	972
Strand Cu:nonCu	1	1	1	1	1	1.6
N. Cu strand (D=1 mm)	360	720	540	1	1	1.6
N. Cu strand (D=1.5 mm)	108	54	162	108	0	108
Jacket thickness [mm]	3.9	5.3	6.8	8.4	10.0	11.7
Turn length [m]	43.92/44.16	44.40/44.64	44.90/45.17	45.44/45.72	46.02/46.34	46.68/47.06
# turns	17/17	17/17	17/17	17/17	17/17	17/15
Hydraulic length [m]	746/751	755/759	763/768	772/777	782/788	794/706

figure 1a, that allows the grading of the SC cross section in the different DLs, depending on the magnetic field, thus optimizing the use of SC. The WP consists of six DLs where the jacket thickness of each conductor increases with the distance from the plasma to withstand the higher mechanical stresses [12]. The originally circular cable-in-conduit conductors (CICCs) are compacted and squeezed to a rectangular shape, see figure 1b, with two low-impedance cooling channels ("holes") [11] delimited by spirals.

Each DL is constituted by a single conductor; the supercritical He at the nominal conditions of 4.5 K and 0.6 MPa is supplied to the two layers of the same DL through a single inlet, so that the He flows in counter-current in adjacent layers. The main geometrical parameters of the conductors are reported in table 1.

3. The 4C model of the TF coil

The 4C model adopted here includes, as in [5], all DLs of the WP (see [13] for details), and the casing, thermally coupled to the WP across the ground insulation and cooled by dedicated CCCs. The casing is discretized in eight poloidal cuts, equally spaced on the inboard (A1-A4) and outboard (B1-B4) legs, see figure 2.

The He inlets are located on the equatorial plane of the outboard leg, on the lateral side of the WP, while the outlets are located on the opposite side, at the same poloidal location. The CCCs inlets are located at the bottom of the coil, as in ITER [14]. Each of the two legs has 48 CCCs connected to inlet / outlet manifolds. We consider here the once-through circulation option [5]. The preliminary design of two cryogenic circuits for the WP and for the casing cooling of [5] is adopted, see figure 2, supplying ~150 g/s to the CCCs circuit and ~60 g/s to the WP (with the target pressure drop of ~1 bar and inlet pressure of ~6 bar during the transient [10]).

The distribution of the magnetic field at End of Flat top (EoF, see below) and nominal operating current (70.8 kA) is reported in figure 1a and 1c, including all contributions from the CS, the Poloidal Field (PF) coils and the plasma. The highest field within the WP is located on the central turns of DL1.1, the innermost layer, at the inboard equatorial plane, while on the outermost DLs the maximum magnetic field is located at the coil sides due to PF contribution, see figure 1a and 1c.

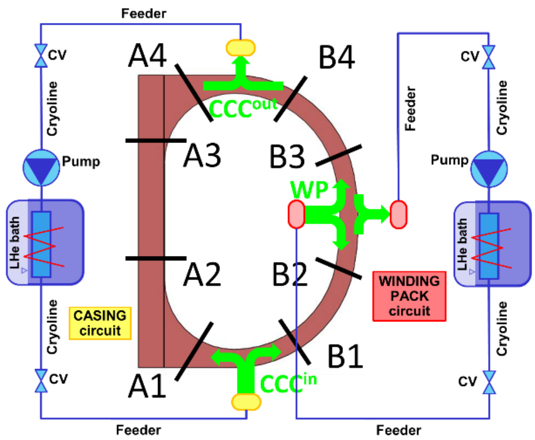

Fig. 2. Schematic representation of the 4C model of the cryogenics circuits for WP (on the right, red manifolds) and CCCs (on the left, yellow manifolds) of the DEMO TF coil. The poloidal cuts A1-4, B1-4 used for the discretization of the casing are highlighted.

4. Simulation setup

The nominal pulsed operation ("normal" operation, case α) consists in a series of standard cycles [15], see figure 3, including a 7200 s plasma burn and ~1800 s dwell time, which are simulated here until periodicity is reached.

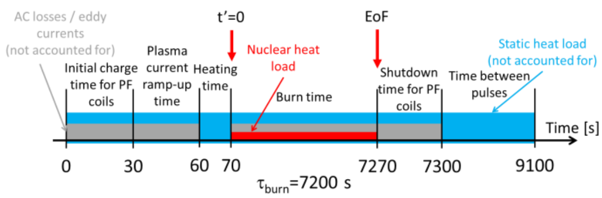

Fig. 3. Evolution of a standard DEMO plasma pulse according to [15].

Only the NH load $P_{NH}(r) = 50\exp(-r/140)$ [W/m^3] is accounted for in both casing and WP in the current analysis, as a function of the radial distance r (in mm) from the plasma facing wall [16], while more detailed NH maps based on Monte Carlo calculations are being prepared and will be implemented in future analyses. The static heat load on the casing surface and the AC/eddy current losses in the conductor/casing during CS and PF coils current ramps are not accounted for.

We then consider also the pulsed operation when the cooling capability in a subset of cooling paths is reduced ("off-normal" operation), and namely the flow is choked:

- in the relief channels of the CICCs with the lowest ΔT_{marg} (DL1.1, DL1.2 and DL6.1), corresponding e.g. to the collapse of one (case β) or both (case γ) spirals, due to the high mechanical stress during the conductor compaction
- in the most critical CCCs, corresponding to the plugging of some CCCs in proximity of the ΔT_{marg}^{min} location in DL1.1 (facing the casing all along its length, case δ), near the outlet of DL2.1 (ΔT_{marg}^{min} for Nb_3Sn DLs, case ζ) and near the outlet of DL6.1 (absolute ΔT_{marg}^{min} location, case η), see figure 4 – a situation that is relevant since the CCCs play an important role in the removal of the NH load, partially contributing also to the cooling of the WP [5].

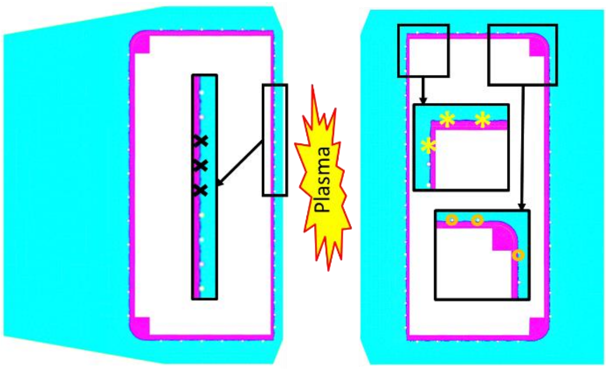

Fig. 4. The CCCs design is shown for both inboard (left) and outboard (right) legs of the coil. Plugged channels are highlighted with crosses for case δ, stars for case ζ and circles for case η.

5. Results

5.1. Normal operation

The periodic behavior in normal operation is reached after two cycles, as shown in figure 5a, reporting the evolution of both the maximum cable temperature and ΔT_{marg}^{min} in DL1.1 (the most loaded conductor). At EoF the ΔT_{marg}^{min} requirement of 1.5 K is satisfied in all the conductors, see figure 5b. Only in DL6.1 (NbTi) it is slightly below the threshold, ~1.43 K, but this is well within the uncertainty on the NH load used in input. In figure 5b it is also shown that, with respect to the initial steady state value, the NH during cyclic operation erodes the initial available ΔT_{marg}^{min} of ~0.1÷0.4 K, depending on the distance from the plasma. Note, however, that the adiabatic condition assumed for the casing surface is not conservative, so that any design for the casing cooling should also be addressed to the static load removal, once a good estimate of it will become available, not to affect and reduce the ΔT_{marg}^{min}.

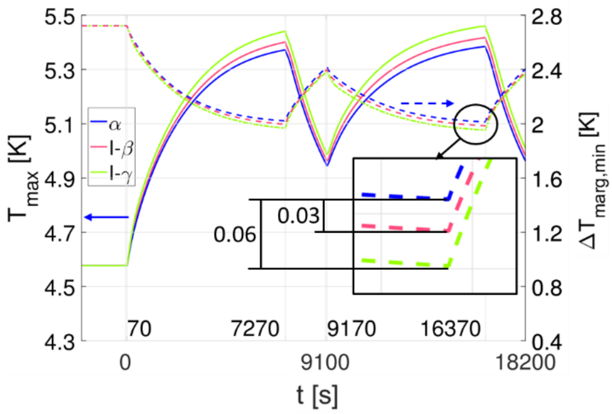

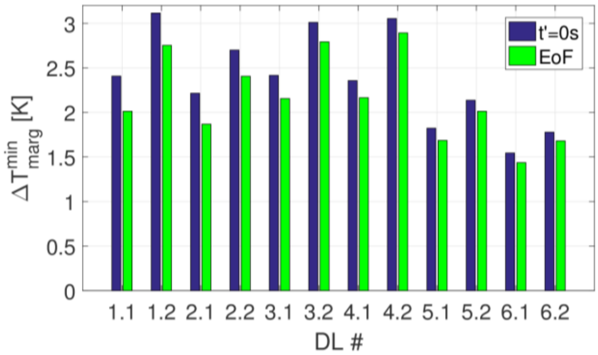

Fig. 5. (a) Evolution of the maximum cable temperature (solid lines, left axis) and of the ΔT_{marg}^{min} (dashed lines, right axis) for case α (blue), β (pink) and γ (green) during the first two cycles, for DL1.1 (case I). (b) ΔT_{marg}^{min} in all layers before the plasma burn start at *t*'=0 s (blue bars), see also figure 3, and at EoF of a periodic pulse (green bars).

5.2. Off-normal operation

The evolution of the $\Delta T_{\rm marg}$ at EoF during the standard plasma burn for both cases I-β and I-γ are reported in figure 5a, where it is compared with the nominal case α, showing that a maximum $\Delta T_{\rm marg}$ reduction <0.1 K is computed, see also table 2, in the worst case (γ), despite a reduction of the mass flow rate >50%. The decrease of the active cooling of the WP is indeed compensated by an increase of the heat transfer to the casing in case of DL1.1, see figure 6, and/or to the neighboring layers.

The effect of CCCs plug on the ΔT_{marg}^{min} in the different cases is also always <0.1 K, as summarized in table 2.

The DL1.1 is, as expected, the most affected by the cooling reduction caused by the CCCs plugging, since it is in contact with the casing all along its length: figure 6 shows the negative heat transfer from the WP to the casing (i.e., the WP is heated by the casing) in correspondence of the plugged CCCs, close to turn #12, for case δ. This is however a conservative situation, as the detachment of the WP from the plasma side of the casing during burn is not taken into account.

6. Conclusions and perspective

The 4C model of an EU DEMO TF coil has been applied to assess the coil performance during standard pulsed operation. The computed ΔT_{marg}^{min} is in line with the design value of 1.5 K assuming the static heat load on the casing surface is negligible. As soon as a good estimate of it will become available, we plan to include it in the analysis and the design of the casing cooling should then be targeted to remove it, not to decrease the WP temperature margin.

Off-normal operating conditions, including the reduction of the available cooling due to collapse of relief channels in the WP and plugging of selected CCCs at critical locations, have also been analyzed, showing that the corresponding erosion of the ΔT_{marg} remains in all cases marginal (<0.1 K).

Table 2. Summary of the ΔT_{marg}^{min} erosion at EoF in the different off-normal operating conditions.

	Case	Temperature margin erosion	
		$\Delta(\Delta T_{\text{marg}})$ [K]	[%]
DL1.1	β	-0.03	-1.4
	γ	-0.06	-3.0
DL2.1	β	-0.02	-1.1
	γ	-0.04	-1.9
DL6.1	β	-0.01	-0.5
	γ	-0.01	-0.7
CCC	δ	-0.08	-3.8
	ζ	-0.04	-1.9
	η	-0.02	-1.5

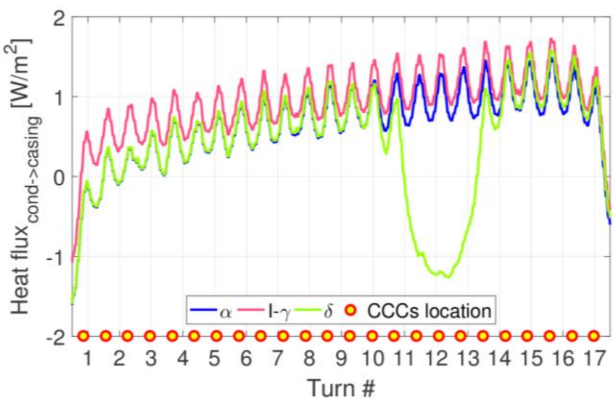

Fig. 6. Heat flux from conductor to casing at cut A3, corresponding to the ΔT_{marg}^{min} location on DL1.1, for cases α (blue), I-γ (pink) and δ (green).

Acknowledgments

This work has been carried out within the framework of the EUROfusion Consortium and has received funding from the Euratom research and training programme 2014-2018 under grant agreement No 633053. The views and opinions expressed herein do not necessarily reflect those of the European Commission.

References

[1] F. Romanelli et al., Fusion electricity. A roadmap to the realisation of fusion energy [Online]. Available: https://www.euro-fusion.org/wpcms/wp-content/uploads /2013/01/JG12.356-web.pdf , accessed on 31 Jul. 2016.

[2] L. Zani et al., Overview of progress on the EU DEMO magnet system design, IEEE Transactions on Applied Superconductivity 26 (4) (2016) 4204505.

[3] L. Zani et al., Overview of Pre-conceptual Design Activities on EU DEMO Reactor Magnet System, presented at ASC 2016 and submitted to IEEE Transactions on Applied Superconductivity.

[4] L. Savoldi Richard, F. Casella, B. Fiori and R. Zanino, The 4C Code for the Cryogenic Circuit Conductor and Coil modeling in ITER, Cryogenics 50 (2010) 167-176.

[5] R. Zanino et al., Development of a Thermal-Hydraulic Model for the European DEMO TF Coil, IEEE Transactions on Applied Superconductivity 26 (3) (2016) 4201606.

[6] L. Savoldi et al., Quench propagation in a TF coil of the EU DEMO, presented at TOFE 2016 and submitted to Fusion Science and Technology.

[7] F. Nunio, TF Magnet system configuration from IDM central database CAD model, EFDA_D_2LMDTE, 04/06/2015, unpublished document.

[8] M. Lewandowska, K. Sedlak and L. Zani, Thermal-Hydraulic Analysis of the Low-T_c Superconductor (LTS) Winding Pack Design Concepts for the DEMO Toroidal Field (TF) Coil, IEEE Transactions on Applied Superconductivity 26 (4) (2016) 4205305.

[9] R. Vallcorba, B. Lacroix, D. Ciazynski, A. Torre, F. Nunio, L. Zani, Q. Le Coz, M. Lewandowska and M. Coleman, Thermo-hydraulic analyses associated with a CEA design proposal for a DEMO TF conductor, to appear in Cryogenics (2016), http://dx.doi.org/10.1016/j.cryogenics. 2016.05.004.

[10] K. Sedlak et al., Common operating values for DEMO magnets design for 2016, EFDA_D_2MMDTG v1.4, 21/06/2016, unpublished document.

[11] L. Muzzi et al., Design, manufacture and Nb3Sn cable-in-conduit conductor with rectangular geometry and distributed pressure relief channels, submitted to IEEE Transactions on Applied Superconductivity (2016).

[12] M. E. Biancolini, Mechanical analysis of TF system, EFDA_D_2MBVLN, 14/05/2015, unpublished document.

[13] L. Savoldi, R. Bonifetto, L. Muzzi and R. Zanino, Analyses of low- and high-margin Quench Propagation in the European DEMO TF Coil Winding Pack, IEEE Transactions on Plasma Science 44 (9) (2016) 1564-1570.

[14] L. Savoldi Richard et al., Mitigation of the Temperature Margin Reduction due to the Nuclear Radiation on the ITER TF Coils, IEEE Transactions on Applied Superconductivity 23 (3) (2013) 4201305.

[15] B. Meszaros, EU DEMO1 2105 Plasma and equilibrium description, EFDA_D_2LJFN7, 18/05/2015, unpublished document.

[16] L. Zani and U. Fischer, Advanced definition of neutronic heat load density map on DEMO TF coils, EFDA_D_2MFVCA, 18/10/2014, unpublished document.